Geology and Ore Deposits at Mineral Park

MOHAVE COUNTY, ARIZONA

William H. Wilkinson, Jr.; Luis A. Vega; and Spencer R. Titley

The Mineral Park mine is a porphyry copper deposit that contains relatively high molybdenum values. Mineral Park, also known as Ithaca Peak, is located approximately 26 km north of Kingman, Arizona in the Cerbat Mountains. The mine occurs in the central part of the Wallapai mining district. The property was acquired by Duval Corporation in 1958, and production of copper and molybdenum concentrates began in October, 1964. Total production through May, 1979, from the Mineral Park mine was 646,398,730 lbs. of copper; 46,795,013 lbs. of molybdenum; and approximately 5,000,000 oz. of silver. Minable reserves at Mineral Park as of January, 1980, were 49,982,000 tons, averaging 0.20 percent copper and 0.051 percent molybdenum.

STRATIGRAPHY AND PETROGRAPHY IN THE MINERAL PARK AREA

The Cerbat Mountains, where the Mineral Park mine is located, are composed of deformed Precambrian metamorphic and igneous rocks (Thomas, 1949) which are intruded by Laramide quartz monzonite porphyry stocks and rhyolite dikes. The rocks of the Cerbat Complex are represented by an older metamorphic group, the amphibolite; a body of gneiss, and younger intrusive rocks. The distribution of these rock types is shown on the mine-area map in Figure 26.1.

Older Rocks

The oldest exposed rocks in the mine area are Precambrian in age and consist of a sequence of quartz-feldspar gneiss, biotite schist, amphibolite, and quartzite. The occurrence of these rocks in folds and their field relationships suggest that they are part of an old sequence of strata. Exposures are discontinuous and evidence of original stratigraphic facing is lacking. The quartz-feldspar gneiss is strongly resistant to erosion and formed the high peaks of Turquoise Mountain and Gross Peak. Eidel and others (1968) have reported that contacts between the quartz-feldspar gneiss and the Laramide quartz monzonite porphyry were often obscured because of alteration. Where they could not make the distinction between gneiss and quartz monzonite they used the term "hybrid." Exposures created by mining have helped to define quartz-feldspar gneiss–quartz monzonite porphyry contacts (see Fig. 26.1) and have indicated that the rocks originally mapped as hybrid are, in fact, quartz-feldspar gneiss. Table 26.1 gives a typical modal composition for the quartz-feldspar gneiss. Plagioclase in the area is too altered to determine compositions.

Amphibolite schists occur throughout the mine, where they are more abundant than the quartz-feldspar gneiss. The amphibolite forms layers which can be traced for up to 5 km. Amphibolite schists are poorly- to well-foliated and characterized by the presence of hornblende. They are dark colored, fine- to medium-grained, xenoblastic rocks. The overall mineralogy varies somewhat, as shown in Table 26.1, where 3 representative modal analyses are listed. Plagioclase is prominently twinned but unzoned. Hornblende has a neutral to blue-green pleochroism in contrast to the brown pleochroism formed in such schists in the surrounding areas (Thomas, 1953).

Biotite schists are minor in volume and variable in composition. They are fine-grained, strongly-foliated, and contain biotite as a major constituent (40–56%). Quartz varies from 10 to 30 percent by volume and plagioclase varies from 0 to 50 percent. Biotite schist is most abundant just north of the Ithaca Peak stock, but it may be present locally throughout the deposit.

The least abundant rock type in the mine area is a fine-grained quartzite. Outcrops are rare, but Thomas (1953) has reported a layer 12 to 15 m thick near Chloride. The

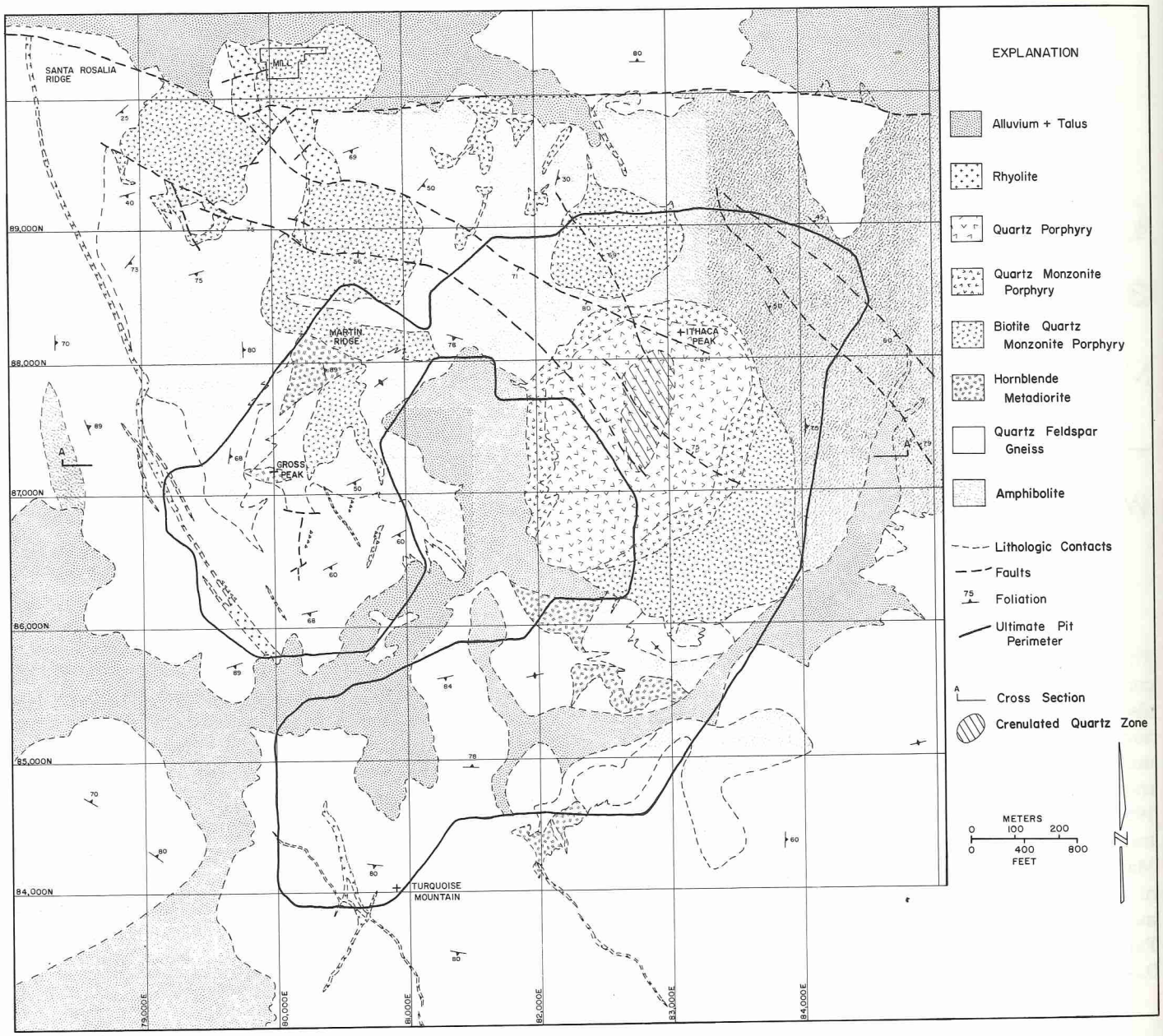

Figure 26.1. Geologic map of the Mineral Park mine area. Most of the rocks of the Wallapi mining district are present in this area.

quartzite has a sugary texture and is garnet-bearing; sparse biotite defines a weak foliation.

Granite Gneisses

The older rocks in the Mineral Park area were intruded by a batholith-sized gneiss complex, varying in composition from biotite quartz monzonite to biotite granite. One of these bodies, the Chloride Granite, has been radiometrically dated (U-Pb) at 1,740 m.y. (Silver, 1967). This age is in agreement with a date (Rb-Sr) derived from similar rocks in the Hualapai Mountains to the south of 1800 ± 470 m.y. (Kessler, 1976). These granite gneisses are the dominant rock types in the Cerbat Mountains, where they form the highest peaks and ridges. The gneisses are medium- to coarse-grained, equigranular rocks in which the development of foliation varies from very strong to indistinct. All of these rock groups are intruded by pegmatites which have been dated (Rb-Sr) from 1,515 to 1,606 m.y. (Wasserburg and Lanphere, 1965).

Diana Granite

The Diana Granite, which locally exhibits weakly developed foliation, is a coarsely porphyritic granite intrusion which has been mapped just west of Chloride. It has been K-Ar dated at 1,350 m.y. (Shafiqullah et al., 1980). The rock is characterized by large (up to 5 cm) orthoclase phenocrysts in a groundmass of orthoclase, microcline, oligoclase, quartz, and biotite (Thomas, 1953). Kessler (1976) has reported data, including Rb-Sr whole rock isochron dates, on 3 plutons of similar lithology in the Northern Hualapai Mountains.

TABLE 26.1
Modal Analyses of Selected Precambrian Rock Samples in the Mineral Park Mine Area

Rock Type	Sample No.	Mineral Composition				
		Quartz	K-feldspar	Plagioclase	Biotite	Hornblende
Quartz Feldspar Gneiss	MP–71	40	45	15	trace	—
Amphibolite Schist	843–1816	23	—	47	5	25
	MP–84	35	—	27	3	35
	905–1012	5	—	40	5	50
Hornblende Metadiorite	843–2734	25	—	50	10	(15)*
	MP–81	25	15	43	5	(12)*
	804–1121	35	20	25	5	(15)*

NOTE: Dash = mineral not present.
* Replaced by secondary biotite.

These plutons are the Hualapai Granite (1,397 ± 69 m.y.), the Holy Moses Granite (1,364 ± 24 m.y.), and an unnamed medium-grained granite (1,337 ± 38 m.y.). This 1,300- to 1,400-m.y.-old intrusive event in the Hualapai and Cerbat mountains is part of the granitic suite recognized by Silver and others (1977) in western North America. These granites and all of the older rocks were intruded by pegmatite dikes dated (Rb-Sr) at 1,100 ± 161 m.y. (Kessler, 1976).

Hornblende Metadiorite

Hornblende metadiorite is the name used at the mine to denote a rock of somewhat variable composition and uncertain age. It is a medium- to coarse-grained, porphyritic-aphanitic, typically non-foliated rock; a weak foliation may be developed adjacent to contacts with other rocks. Near its contacts with amphibolite, fragments of foliated amphibolite schist are often observed.

The distribution of hornblende metadioriate is restricted to the immediate area of the mine and to an area northwest of the mine. The occurrence of hornblende metadiorite only near the Laramide intrusive rocks led Eidel and others (1968, p. 1262) to speculate that the hornblende metadiorite was "metasomatized schist that has been partially remobilized." Several relationships point to an alternate interpretation. The contacts of hornblende metadiorite with other rocks, especially with amphibolite schist, frequently show small-scale interfingering of hornblende metadiorite into the schist along foliation planes; on a larger scale the hornblende metadiorite is commonly discordant to Precambrian foliation. Fragments of foliated amphibolite schist are common in the hornblende metadiorite adjacent to schist contacts. Near these contacts there is often a grain size variation in the hornblende metadiorite from fine-grained near the contacts to increasingly coarser-grained away from the contacts. Together all of these features strongly indicate an intrusive origin for the hornblende metadiorite.

Because the metadiorite is not foliated but intrudes foliated Precambrian rocks, the rock is younger than the last metamorphic event. The hornblende metadiorite is intruded by quartz monzonite porphyry and is, therefore, older than the Laramide porphyry. The petrographic differences between quartz monzonite porphyry and hornblende metadiorite (Table 26.2) further serve to separate these two rock types. The intrusion of the hornblende metadiorite by pegmatites—the documented, widespread 1,300- to 1,400-m.y.-old intrusion event—and the similarity of the hornblende metadiorite to one of Kessler's (1976) 1,300- to 1,400-m.y.-old plutons provide substantial reason to include the hornblende metadiorite as one of the Younger Precambrian plutons.

Laramide Rocks

Biotite quartz monzonite porphyry, biotite quartz diorite porphyry, and rhyolite dikes compose a group of intrusive rocks localized at the Mineral Park mine. A K-Ar age of 71.5 ± 2.6 m.y. (Mauger and Damon, 1965) on vein biotite from Ithaca Peak establishes a Laramide age for early stages of alteration. This date represents a minimum age of intrusion. Rhyolite dikes crosscut the biotite quartz monzonite and quartz diorite porphyries but, in turn, are cut by mineralization and, thus, they may be genetically related to the stock intrusions.

The biotite quartz monzonite porphyry and biotite quartz diorite porphyry are discrete intrusions. Although there is no direct evidence for a connection of these bodies, their "stratigraphic" position in the intrusion-mineralization

TABLE 26.2
Petrographic Differences Between Hornblende Metadiorite and Biotite Quartz Monzonite Porphyry in the Mineral Park Mine Area

Hornblende Metadiorite	Biotite Quartz Monzonite Porphyry
1. Never has aplitic groundmass	1. Often has aplitic groundmass
2. Plagioclase is sharply twinned but *not zoned*	2. Plagioclase is twinned and is *strongly zoned*
3. Contains 5 to 15 percent biotite	3. Contains 2 to 10 percent biotite
4. Biotite is irregular, frayed, clotted	4. Biotite is in books with frayed ends and as isolated grains
5. Hornblende present up to 15 percent, although normally altered to biotite	5. No hornblende
6. Plagioclase is anhedral to subhedral, never euhedral	6. Plagioclase is euhedral to subhedral, often as isolated, euhedral grains

sequences indicates that they represent the same intrusive event. They occur as two main masses, the Ithaca Peak stock and the Gross Peak stock.

Ithaca Peak Stock. The Ithaca Peak stock is a single intrusion of quartz monzonite composition that passively intruded the Precambrian Cerbat Complex (Stringham, 1966). It shows concentric zoning of igneous rock types which range from biotite quartz monzonite porphyry at the contact to quartz porphyry at the center. An intermediate zone called quartz monzonite porphyry is mapped at the mine, but is distinguished from the biotite quartz monzonite porphyry only by the sericitization of biotite. The areal extent of this zone of sericitized biotite diminishes with depth, and the bottom of sericitization coincides with the bottom of chalcocite enrichment. These features suggest that the rock mapped as quartz monzonite porphyry is not a separate rock type, but is instead the product of supergene alteration of the biotite quartz monzonite porphyry.

The biotite quartz monzonite porphyry is a medium-grained, porphyritic-phaneritic to porphyritic-aphanitic rock, with compositions as shown in Table 26.3. The phenocryst phases are euhedral to subhedral; plagioclase is twinned and well zoned with compositions ranging from An_{24} to An_{30}. Rutile, apatite, and zircon are accessory minerals. Two whole rock chemical analyses of the freshest available biotite quartz monzonite porphyry are given in Table 26.4. Although these rocks appear fresh, they contain a high S content, indicating that they are mineralized.

The quartz porphyry is restricted to the central portion of the Ithaca Peak stock, where it forms an elliptical zone with a northeast axis approximately 600 m long and a northwest axis approximately 425 m wide. The quartz porphyry has a quartz monzonite composition, but it is texturally distinct from all other Laramide rocks at Mineral Park. The quartz porphyry is characterized by large (up to 1.5 cm), rounded and embayed quartz "eyes," plagioclase, biotite, and occasional large (up to 4 cm) K-feldspar phenocrysts in an aplitic groundmass. Plagioclase is twinned and well zoned, with compositions ranging from An_{24} to An_{30}.

Near the center of the quartz porphyry is an elliptical core approximately 210 m by 150 m that contains zones of crenulated quartz and large quartz pods, up to 40 m high and 12 m wide. The crenulated quartz veins are sinuous, often tightly folded bands of quartz that cut the matrix of the quartz porphyry but not the phenocrysts. These veins are similar to those described at Henderson (Wallace et al., 1978), though at Mineral Park the veins occur near the center of the quartz porphyry, rather than near the contacts of intrusive phases as at Henderson.

Variations in the original igneous textures of the stock enable recognition of three different textural/lithologic types: (1) seriate-granitic biotite quartz monzonite porphyry, (2) porphyritic-aplitic biotite quartz monzonite porphyry, and (3) porphyritic-aplitic quartz porphyry. The porphyritic-aplitic texture is the most widespread and is developed in two different rock types. This texture is characterized by phenocrysts of quartz, plagioclase, biotite, and K-feldspar in a fine-grained, sugary-textured groundmass that consists of an interlocking mosaic of quartz, orthoclase, and minor biotite.

The distribution of these textural types is shown in Figure 26.2. The seriate-granitic phase forms an incomplete zone 31 to 152 m wide around the southern and eastern margins of the Ithaca Peak stock. The aplitic phases occupy the cen-

TABLE 26.3
Modal Analyses of Selected Laramide Rock Samples From Ithaca Peak and Gross Peak Stocks

	Rock Type	Sample No.	Phenocrysts				Groundmass			
			Plagioclase	Biotite	Quartz	K-feldspar	Quartz	K-feldspar	Biotite	Plagioclase
Ithaca Peak	Seriate Biotite Quartz Monzonite Porphyry	MP–63	50	10	5	±2	17	15	—	—
	Aplitic Biotite Quartz Monzonite Porphyry	MP–93	35	4	4	±1	30	25	±2	—
	Aplitic Quartz Porphyry	MP–61–II	20	3	10	±2	23	28	—	13
Gross Peak	Biotite Quartz Monzonite Porphyry	MP–74	45	10	5	—	20	17	3	—
	Biotite Quartz Diorite Porphyry	MP–27	55	3	5	—	25	12	—	—
	Biotite Quartz Monzonite Porphyry Dike	MP–17	40	10	1	—	21	25	3	—

NOTE: Dash = mineral not present.

TABLE 26.4
Whole Rock Chemical Analyses of
Biotite Quartz Monzonite Porphyry From Ithaca Peak Stock

Compound/Element	Sample Number		Average
	MP-78	MP-80	
SiO_2	72.2	71.6	71.9
Al_2O_3	14.7	15.5	15.1
TiO_2	0.036	0.11	0.073
CaO	1.68	2.10	1.89
MnO	0.03	0.01	0.02
MgO	0.71	0.73	0.72
Fe_2O_3	3.35	3.15	3.25
Na_2O	3.37	3.10	3.24
K_2O	3.73	2.89	3.31
S	1.94	1.34	1.64
Less on Ignition	3.0	2.14	2.57
Total	104.75	102.67	103.71
Be (ppm)	3	2	2.5
Cu (ppm)	585	635	610
Mo (ppm)	35	5	20
Pb (ppm)	15	10	12.5
Zn (ppm)	55	85	70
Ni (ppm)	5	5	5
Cr (ppm)	15	15	15
V_2O_5 (ppm)	80	110	95

NOTE: Analyses by Rocky Mountain Geochemical Corp., using atomic absorption.

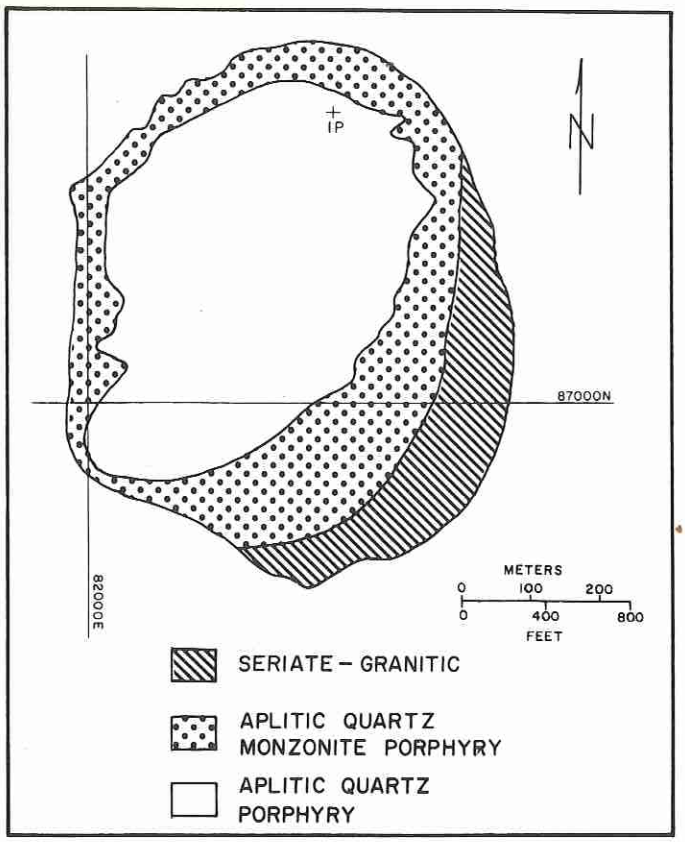

Figure 26.2. Distribution of textural types in the Ithaca Peak *(IP)* stock

tral portions of the stock, with the quartz porphyry in the center. There is textural gradation among the different phases, and the contacts between the two biotite quartz monzonite porphyry phases are not recognizable in exposures at the mine. The contact between biotite quartz monzonite porphyry and quartz porphyry is sub-vertical and gradational over 1 to 2 m. This contact is marked by a gradual disappearance of quartz eyes in the quartz porphyry. Aplites are common near the biotite quartz monzonite porphyry–quartz porphyry contact and in some cases may actually mark the contact. At one location the contact is marked by a fault.

Eidel and others (1968) have recognized this distribution of lithologic types. They have interpreted the zoning to be the result of crystallization of an equigranular rind, with development of the porphyritic texture caused by the fracturing of the pluton and the release of volatiles that produced rapid crystallization in the center of the stock. They have attributed formation of the aplites to injection of some of the rapidly crystallizing liquid along the contacts and into the biotite quartz monzonite porphyry. Similar interpretations for similar textural zoning have been presented by Nielsen (1968) for the Santa Rita stock and by Graybeal (1972) for the Patagonia Batholith.

The contacts of biotite quartz monzonite porphyry and Precambrian rocks are typically very sharp, with no observable thermal effects. Eidel and others (1968) have reported xenoliths of Precambrian schist in the porphyry adjacent to the contacts, but these xenoliths are uncommon at deeper levels of exposure in the mine. Dikes of biotite quartz monzonite porphyry in the Precambrian rocks are common, especially along the northern margin of the Ithaca Peak stock. Dikes of biotite quartz monzonite porphyry have been observed in drill core samples of Precambrian rocks as far as 150 m away from the contact. Bench maps of higher levels indicate that dikes were more common and widespread at higher elevations. Eidel and others (1968) have suggested that the Ithaca Peak stock had an inverted tear-drop shape. Recent drill data indicate that the contacts are irregular and dip sub-vertically.

Gross Peak Stock. The rocks grouped as the Gross Peak stock occur on Martin Ridge, under the mill site, and on Santa Rosalia Ridge (see Fig. 26.1). Most of the discussion in this section concerns the portion of the stock exposed along Martin Ridge, because the quartz monzonite porphyry on Santa Rosalia Ridge and under the mill site are too altered to yield usable samples. Two petrographically distinct rock types, separable only on the basis of microscopic study, make up the Gross Peak stock: biotite quartz monzonite porphyry and biotite quartz diorite porphyry. In thin section the only distinction is in differing amounts of groundmass K-feldspar (see Table 26.3). Plagioclase in both rocks is well zoned, with compositions ranging from An_{25} to An_{35}. The biotite quartz monzonite porphyry from Gross Peak is finer-grained and more biotite-rich than that from the Ithaca Peak stock.

Cross sections indicate the the intrusion on Gross Peak south of 88,000N (Fig. 26.1) is keel-shaped in an east-west direction (Fig. 26.3*A*). It pinches out to the south into 2 large, finger-like projections and, thus, is sill-like from the larger mass to the north. There are no drill data to provide information on the vertical extent of the northern part of the

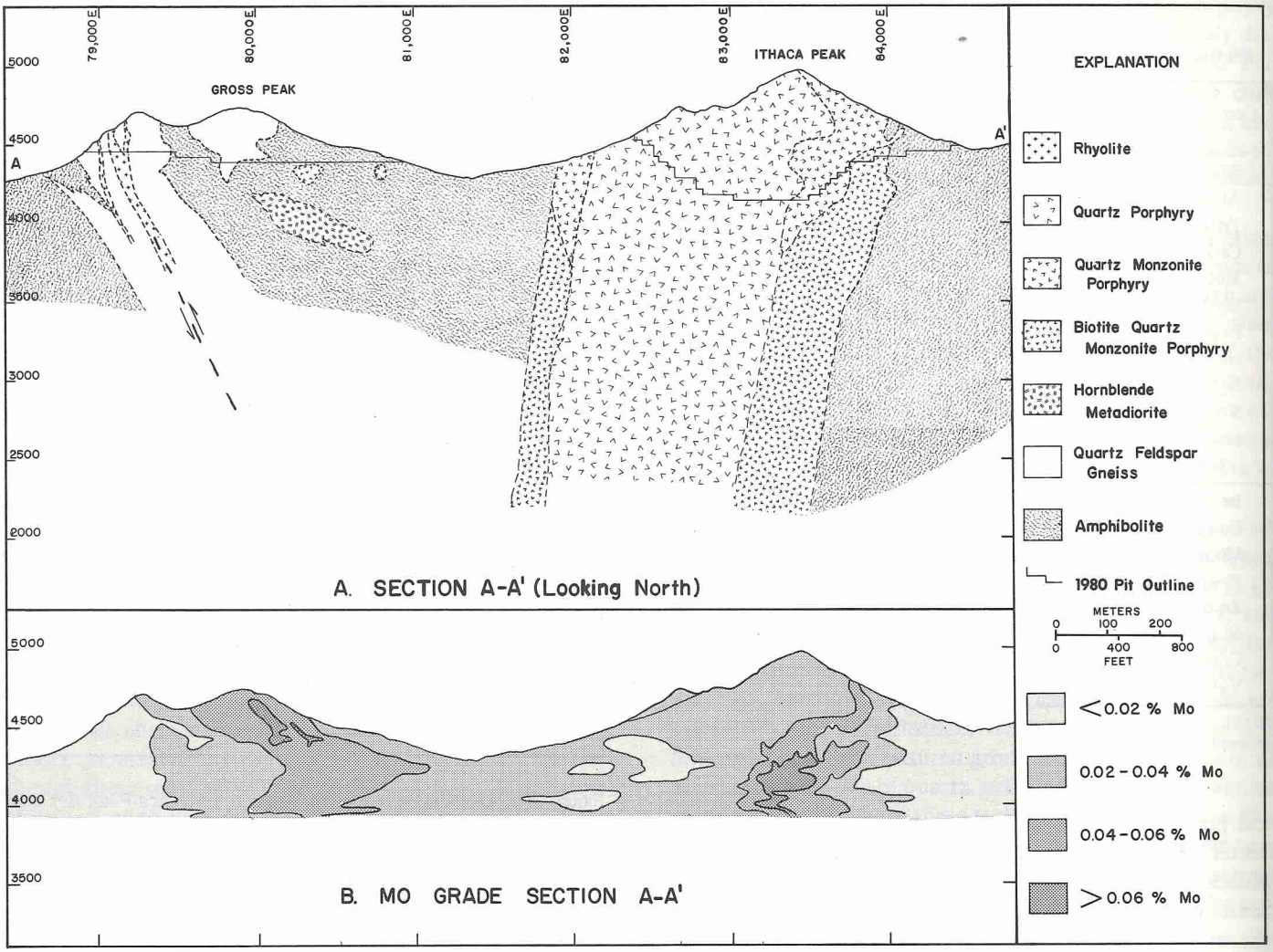

Figure 26.3. Cross sections in the Ithaca Peak–Gross Peak area: *A,* rock distribution at section *A-A'* (looking north); *B,* molybdenum grades at section *A-A'*. Location of section shown in Figure 26.1.

biotite quartz monzonite porphyry. South of 87,000N, several small, north-trending biotite quartz monzonite porphyry dikes were exposed during mining (see Fig. 26.1). These dikes appear to extend to the north into the sill-like mass of the Gross Peak stock. Texturally and compositionally (see Table 26.3) these dikes are identical to the biotite quartz monzonite porphyry to the north.

Rhyolite Dikes. The last intrusive event in the mine area resulted in the emplacement of aphanitic rhyolite dikes. These rocks are white to light pink and only rarely contain small K-feldspar or quartz phenocrysts. The dikes have sharp contacts and typically exhibit flow-banding adjacent to the contacts. The rhyolite dikes cut the biotite quartz monzonite porphyry along Santa Rosalia Ridge and are in turn cut by mineralization. The intrusions at Mineral Park occur at the approximate geographic center of the area containing rhyolite dikes. This coincidence of intrusions and rhyolite dikes and their similarity of ages suggest that they are genetically related.

Breccia Dikes. Several breccia dikes have been noted in bench faces and drill core samples in the Gross Peak area. They are quite erratic in trend, although north-south appears to be a preferred orientation. Commonly they occur along the contacts of biotite quartz monzonite porphyry and rhyolite dikes. The average thickness of the breccia dikes is .5 m, but they range from 1 cm to 6 m.

Angular to sub-rounded fragments occur randomly in a fine-grained matrix that has been strongly altered to secondary biotite, K-feldspar, and quartz. The fragments consist of all the rock types found at the mine except the Laramide porphyries. The breccia dikes are pre-mineral, but their exact relation to the rhyolite and biotite quartz monzonite dikes is problematic. Although the rhyolite cuts the monzonite, only fragments of the rhyolite occur in the breccia dikes. A better understanding of the sequence of events must await an exposure exhibiting definitive relations among the three events.

STRUCTURE OF THE WALLAPAI MINING DISTRICT

The structural evolution of the Cerbat Mountains, where the Wallapai mining district is located, is long and complex. As no Paleozoic rocks remain, structural interpretations are based largely upon discontinuous and incomplete records

from the Precambrian rocks. Laramide rocks provide the only record in the gap between Precambrian and mid-Tertiary time. It is not the intent of this study to interpret the regional geologic setting, but an understanding of the structural history of the Wallapai mining district is essential to an understanding of the geologic history at Mineral Park. Because of widespread exposures of Precambrian rocks, and because of the position of the Mineral Park intrusion complex in that terrane, the district affords an excellent opportunity to examine the possible basement influence on control of porphyry mineralization.

The Wallapai mining district is approximately 6.5 km wide and 18 km long and is defined by the known lateral extent of base and precious metal veining (Fig. 26.4). The Ithaca Peak intrusions occur at the geographic center of the district. Orientations of Precambrian foliation vary within the district and define a series of open folds in the older Precambrian rocks. Faulting is expressed as fault-veins and silicified zones, but the lack of marker units precludes determination of offset. Mineralized fractures are important structural elements in the mine area.

Foliation and Folds

Foliation in the Precambrian rocks of the Wallapai mining district is defined by the alignment of biotite in schistose and granitic rocks and by gneissic layering in the granitic gneisses and quartz-feldspar gneiss. Based on foliation trends, the district can be divided into two distinct domains —one in which foliation has a regional northeast trend and one which expresses variable foliation trends. In the first domain there is a strong N40° to 70°E–striking foliation with steep dips. Although there are local variations in attitudes, this trend is present throughout the eastern parts of the Cerbat and Hualapai mountains. This foliation pattern is developed wholly within the batholithic granitic gneisses.

The domain of variable foliation trends is restricted to the western flank of the Cerbat Mountains and involves only the older Precambrian rocks. This domain extends from just north of Chloride at least to the old camp at Cerbat. The foliation within this domain is concordant with lithologic layering and defines a series of steep, rather open synforms and antiforms. Three such series of folds have been identified: (1) the Chloride fold, (2) the Roper Ridge and Turquoise Mountain folds, and (3) the Todd Basin folds (see Fig. 26.4).

The contact between the two structural domains is defined largely by changes in foliation directions and, locally, by lithologies. The structural characteristics at this contact are best observed west of the Keystone Mine (see Fig. 26.4). The number of inclusions of amphibolite in the granitic gneiss increases westward toward the contact. West of the Keystone Mine there is an area of high concentration of amphibolite and schist inclusions in a migmatite zone, and foliation trends are chaotic. Adjacent to the contact, foliation in the amphibolite inclusions in the granitic gneiss still follows the trend of the Roper Ridge fold. To the east, away from the contact, these foliations are gradually rotated until foliation in the amphibolite inclusions parallels foliation in the granitic gneiss.

These characteristics of foliation and the abundance of inclusions of amphibolite in the granitic gneiss suggest that the granitic gneiss intruded an already-folded sequence of meta-sedimentary and meta-volcanic rocks. Folds present are interpreted as remnants of folded terrain that was once more widespread.

The contact between the two domains extends over the distance from Chloride to Cerbat; although the contact is often irregular, its general trend is N30°W. It is noteworthy that both the Ithaca Peak and Alum Wash mineralized centers lie along or near this contact, which is also the locus of major veins and rhyolite dikes in the district. At a point just northwest of Mineral Park, the northernmost major dike makes an abrupt turn to a N25°E trend, and a N10°E strand also diverges from the main group at Todd Basin south of the mine; however, most of these dikes form a series of N30°W-trending swarms that reach a thickness of 30 m (see Fig. 26.4). Thus, although there is no structural break observed on the ground, the contact between the two domains appears to have controlled emplacement of intrusions in the Wallapai mining district.

Faults

Faults are abundant in the district, but the lack of good marker units makes offset and age relationships difficult to interpret. There is evidence that many of the rhyolite dikes were intruded along pre-existing structures. A major fault of probable regional extent occurs west of Gross Peak, where it marks the western edge of mineralization (Fig. 26.1). This fault, named here the Gross Peak fault, is marked by a large rhyolite dike as well as by change in attitudes of foliation in the Precambrian rocks on either side. Eastward, along the trace of the Turquoise Mountain fold limb, the strike of the foliation rotates to east-west around the nose of the fold with dips to the north. The strike of foliation continues across the fault, but dips are rotated from a northerly to a southerly direction at the fault. Cross sections indicate that there is up to 425 m of reverse movement on the Gross Peak fault, with the east side up.

The most obvious faults are those structures which form the major veins of the district. These fault-veins are younger than the rhyolite dikes that they cut. Fault-veins of the district are generally planar to gently curving and form systems of sub-parallel veins. The veins show consistent strikes from N30° to 60°W, with mostly steep dips, although the strikes of veins near Chloride depart from the regional trend and follow the limbs of the Chloride fold. Physical descriptions of these veins are presented by Thomas (1949, 1953) and Dings (1951).

Figure 26.4 shows the distribution of fault veins with an outline envelope drawn around their maximum extent. The long axis of this envelope has a N30°W trend. The majority of the veins occupy the central portion of this envelope; the major groups of veins and the axis of the envelope are centered on the Precambrian contact.

Several large faults are present in the area from Roper Ridge to Ithaca Peak (Fig. 26.4) and near the mill site. Roper Ridge, Santa Rosalia Ridge, and Ithaca Peak (Fig. 26.1) are aligned along a N70°W fault zone. The major bordering faults are shown on Figure 26.1, but between these faults there are numerous smaller faults, together with zones of intense fracturing and silicification. Such silicification has

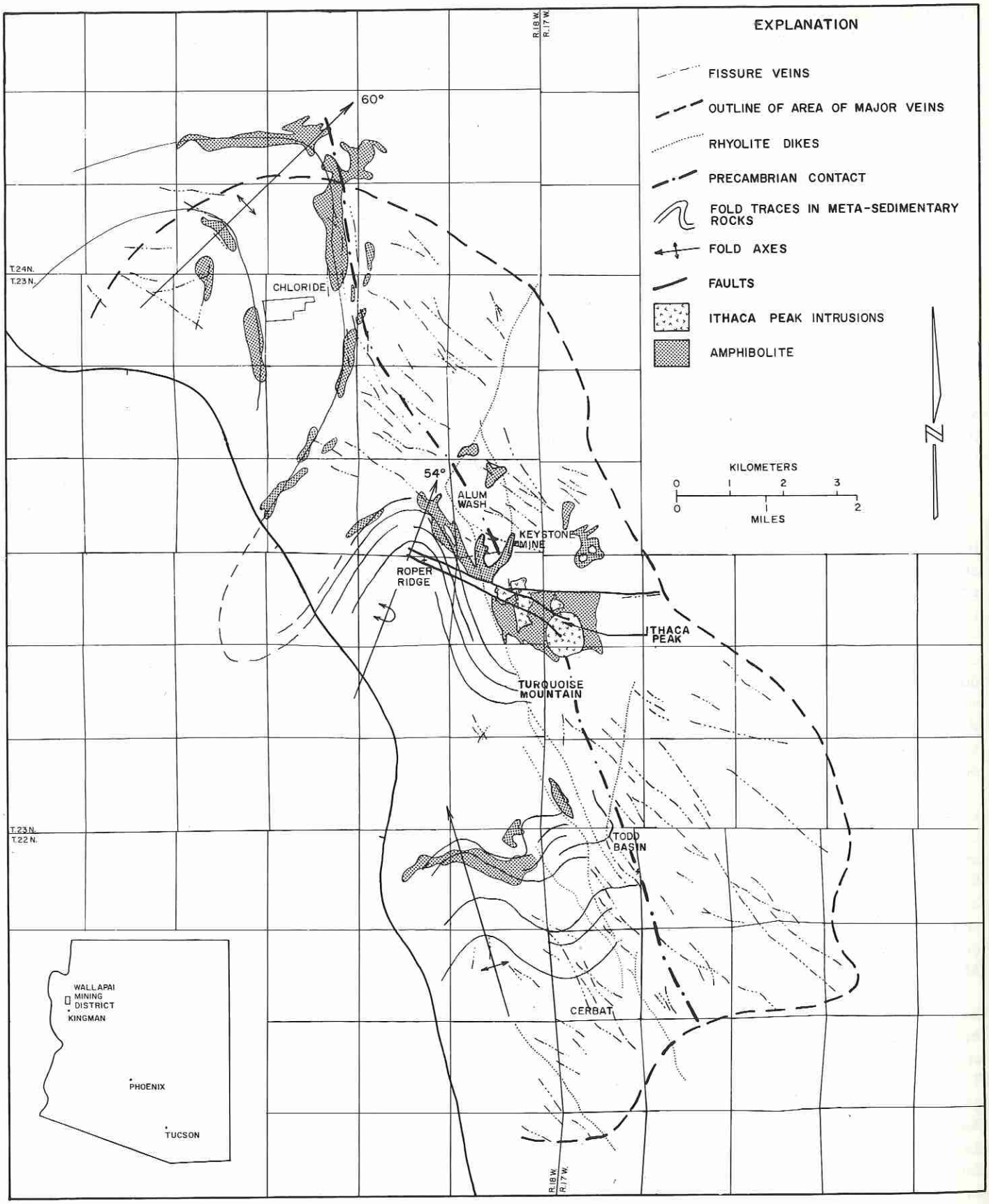

Figure 26.4. Generalized geologic and structural map of the Wallapai mining district

created the resistant masses of ridges and peaks at Mineral Park. Near the mill site, an east-striking strand of this zone of faulting is developed and can be traced eastward. The fault zone marks the sharp change from amphibolite schist to quartz-feldspar gneiss north of Ithaca Peak (see Fig. 26.1).

Summary of Major Structural Features

A brief chronological summary of the major structural features of the Wallapai mining district is given below:

1. A screen of folded meta-sedimentary and meta-volcanic rocks occurs along the western flank of the Cerbat Mountains.
2. The folded rocks are intruded by a regionally northeast-foliated granitic gneiss of batholitic proportions.
3. The contact between the folded rocks and the granitic gneisses becomes a major structural element in the district.
4. Intrusion of the Ithaca Peak stocks appears to localize at the intersection of this contact and the Turquoise Mountain fold.
5. The contact is the locus for intrusion of rhyolite dikes and for formation of the major fault-veins of the district.

ALTERATION AND MINERALIZATION IN THE MINERAL PARK DEPOSIT

Hydrothermal alteration associated with the Mineral Park deposit is structurally controlled and has evolved through different stages. Each stage has superimposed its characteristic alteration assemblage on successively earlier stages of alteration. This has resulted in a complex, though systematic, distribution of alteration types for which a paragenetic sequence can be determined. The extensive development of supergene alteration has complicated the alteration picture, but increasing depth in the pit has allowed direct observation of rocks below the base of supergene alteration. This asset, combined with deep drilling, has aided in the separation of hypogene from supergene effects.

Two types of alteration are recognized at Mineral Park: selectively pervasive and veinlet controlled. The characteristics of all the recognized alteration assemblages at Mineral Park are given in Table 26.5 and their paragenetic sequence is shown in Figure 26.5.

Selectively Pervasive Alteration

Selectively pervasive alteration occurs in large rock volumes but affects only certain minerals in the host rock (Titley, 1978). A widely recognized selectively pervasive type of alteration is the replacement of hornblende and primary biotite by secondary biotite. This type is the earliest alteration event recognized at Mineral Park. Secondary biotite is present over an area approximately 1.7 km by 1.45 km (Fig. 26.6); in this area it replaces hornblende in Precambrian amphibolite schist and is present in biotite quartz monzonite porphyry due to recrystallization and to partial pseudomorphic replacement of primary biotite.

Secondary biotite is most easily recognized in the Precambrian amphibolite schists and hornblende metadiorite, where hornblende is partially to totally replaced by aggregates of fine biotite flakes plus quartz and magnetite. At least partial replacement of hornblende was observed in nearly every thin section of the Precambrian rocks examined. Biotite replacement of primary biotite is never total; replacement textures are limited to felty biotite rims around the edges of biotite phenocrysts. The most characteristic feature is the development of a sagenitic rutile texture. A less common manifestation of secondary biotite is the occurrence of scattered, small flakes of biotite in the groundmass of the quartz porphyry and biotite quartz monzonite porphyry. The most abundant secondary biotite observed at Mineral Park, pervasive plus veinlet controlled, occurs at the outer edge of the low-grade copper core. This distribution of secondary biotite is similar to that observed by Carson and Jambor (1974) at Babine Lake, Canada, and by Phillips and others (1974) at the Ray, Arizona, deposit.

A second selectively pervasive alteration assemblage is the rimming and partial to total replacement of plagioclase by K-feldspar. The final result, complete conversion of plagioclase to K-feldspar, was observed in all rock types, but is not as widespread as secondary biotite. K-feldspar may in part be veinlet controlled, but it is pervasive over areas of tens of meters in core samples and in bench faces.

Veinlet-Controlled Alteration

The major portion of alteration effects observed at Mineral Park can be directly attributed to alteration along veins and veinlets. The alteration assemblages may occur either within veinlets or as halos adjacent to veinlets. A paragenetic sequence for these assemblages can be established in terms of evolution through time based on crosscutting relationships (see Table 26.5). Two enigmatic, discordant features—quartz pods and crenulated quartz veins—are not included in the paragenetic sequence because of the lack of crosscutting relationships with other vein types. Sulfides are not associated with these features.

The biotite and K-feldspar veinlets are usually irregular, contain little quartz, and may extend for tens of meters. Biotite and K-feldspar are stable with respect to each other, and biotite, though not obvious in hand specimens, is usually present in K-feldspar veinlets. The K-feldspar veinlets have diffuse contacts with the wall rocks. K-feldspar veining and flooding is essentially co-extensive with, but in part younger than, secondary biotite (see Fig. 26.6).

The coarse-grained quartz-biotite vein assemblage has been observed in two places; in one of these a biotite vein marks the eastern contact of the biotite quartz monzonite porphyry with Precambrian rocks in the Ithaca Peak stock. The vein reaches half a meter in width and consists of intergrown, coarsely crystalline biotite and quartz. There is abundant evidence for the later introduction of quartz into the vein. Sulfides that are present replace biotite and may be related to introduction of the later quartz.

Table 26.5 and Figure 26.5 show two molybdenite-bearing vein sets, one of which is quartz-molybdenite and the other, quartz–K-feldspar–anhydrite–molybdenite. There are sufficient differences in homogenization temperatures, as well as in alteration assemblages, to separate these types in time.

TABLE 26.5
Characteristics of Alteration Vein Assemblages by Rock Type at Mineral Park

	Alteration Type	Biotite Quartz Monzonite Porphyry/Quartz Feldspar Gneiss	Amphibolite Schist	Hornblende Metadiorite
Selectively Pervasive	Biotite	Recrystallization of magmatic biotite with formation of sagenitic rutile Partial replacement of primary biotite along edges Scattered small flakes and clots	Replacement of hornblende by biotite + quartz + magnetite + carbonate Replacement of primary biotite by felty biotite around edges + minor rutile Occasional biotite along fractures and cleavage in plagioclase	Replacement of hornblende by biotite + quartz + magnetite—more complete than in amphibolite Replacement of primary biotite by felty biotite around edges + minor rutile
	K-feldspar	Rimming and partial to total replacement of plagioclase Less abundant than biotite	Some replacement of plagioclase, but may be veinlet-controlled	Rimming and partial replacement of plagioclase Replaces biotite
Veinlet Controlled	Biotite	Veinlets	Replaces hornblende adjacent to veinlets	
	K-feldspar	Diffuse veinlets; replaces wall rock adjacent to veinlets	—	—
	Quartz + K-feldspar + Biotite + Anhydrite + Pyrite + Molybdenite	K-feldspar selvages Sparse carbonate	Biotite replaces hornblende and primary biotite adjacent to veinlets Sparse carbonate	
	Quartz + Molybdenite + Pyrite	No alteration Molybdenite restricted to veinlets	Biotite replaces hornblende Molybdenite restricted to veinlets	Molybdenite restricted to veinlets
	Quartz + Chalcopyrite + Pyrite + Chlorite ± Magnetite + K-feldspar ± Epidote ± Anhydrite	Chlorite in veinlets and replacing biotite adjacent to veinlets Contains minor sphalerite and galena 10% chalcopyrite in mafic sites in halo adjacent to veinlets	Chloritization of biotite adjacent to veinlets Contains minor sphalerite and galena Albite occurs with some of these veinlets 10% chalcopyrite in mafic sites in halo adjacent to veinlets	
	Quartz + Pyrite + Sericite ± Carbonate	Plagioclase and biotite replaced by sericite adjacent to veinlets Wide sericite halos	Chloritization of primary and secondary biotite Carbonate greater than sericite Plagioclase replaced by sericite and carbonate Minor epidote	
	Complex Veins	1. Formation of chlorite + pyrite + epidote + sericite + clay 2. Silicification and white mica adjacent to vein 3. Sericite + clay + sphene replace (1) and (2) (Thomas, 1949)	—	—

NOTE: Vein types are listed in paragenetic order, with oldest at the top and youngest at the bottom. Dash = mineral assemblage not observed.

An identical sequence of early molybdenite + K-feldspar followed by quartz + molybdenite has been described at Butte (Brimhall, 1977).

The chalcopyrite-bearing veins are poorly exposed in the pit, and little is known about them because of supergene replacement of chalcopyrite by chalcocite. The characteristics of chalcopyrite-bearing veins summarized in Table 26.5 were obtained mostly from drill core data supplemented by some observations in the lowest portions of the pit. It is noteworthy that magnetite and chalcopyrite are contemporaneous in these veinlets. The distribution of magnetite in the pit and in drill hole samples falls within the high copper zone similar to distributions at Ray (Phillips et al., 1974). Another important feature of chalcopyrite-bearing veinlets is that the first paragenetic occurrence of chlorite is observed as a phase of this veinlet alteration assemblage. Chlorite occurs as grains in the veinlets or replaces secondary and primary biotite adjacent to the veinlets.

Quartz-pyrite-sericite veinlets represent the last important mineralizing event in the pit and have the greatest degree of development in the more felsic rocks. In the more mafic rocks, sericite is less common; calcite, chlorite, and very minor epidote take its place.

Studies of polished sections indicate that the molybdenite-bearing veinlets contain no observable chalcopyrite except where reopening can be demonstrated. The chalcopyrite veinlets, however, consistently show minor amounts of sphalerite. The quartz-pyrite-sericite veinlets contain pyrite as the dominant sulfide, though very minor amounts of chalcopyrite may be present. Locally, where quartz-pyrite-sericite veinlets cut quartz-molybdenite veinlets, molybdenite is contained in the quartz-pyrite-sericite veinlets, but the amount rapidly diminishes within several centimeters away from the veinlet intersections.

The final major stage of sulfide deposition is represented by the complex quartz-chalcopyrite-pyrite-sphalerite-galena veins, which form the major veins in the Wallapai mining district. These veins cut all other vein types in the pit, but they are of only local importance at the mine. These veins reach widths of 16 m in other parts of the district.

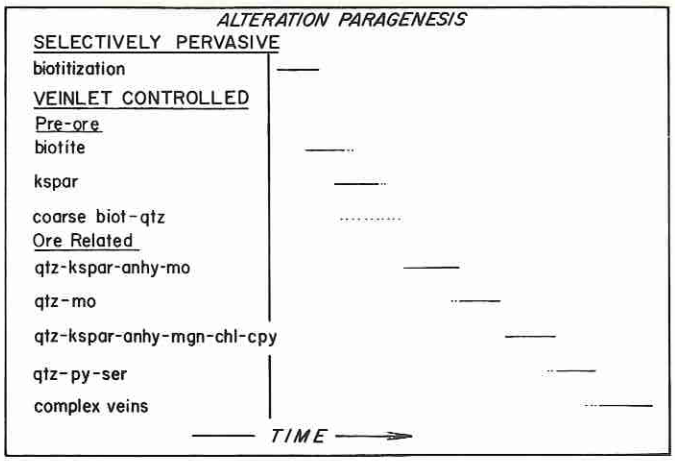

Figure 26.5. Paragenesis of major alteration assemblages at Mineral Park mine. Key: *anhy* = anhydrite, *biot* = biotite, *chl* = chlorite, *cpy* = chalcopyrite, *kspar* = K-feldspar, *mgn* = magnetite, *mo* = molybdenite, *py* = pyrite, *qtz* = quartz, *ser* = sericite.

Distribution of Alteration and Mineralization

Each successively younger alteration assemblage at Mineral Park overlaps and crosscuts earlier alteration assemblages. This relationship is most apparent between early potassic alteration, pervasive and veinlet biotite and K-feldspar alteration, and late quartz-pyrite-sericite alteration. Potassic alteration assemblages recognized in the pit and in drill core samples are extensive (see Fig. 26.6). The quartz-pyrite-sericite assemblage, which completely overprints the volume of potassic alteration, is also abundant throughout the deposit; further, this alteration type extends up to several hundred meters beyond the limits of potassic alteration. At the levels exposed in 1981 no discrete quartz-sericite "shell" (Lowell and Guilbert, 1970) was present.

Diamond drilling and rock chip geochemistry have provided data on which the lateral distribution of molybdenum and copper mineralization may be defined. In Figure 26.7 the 0.01 percent molybdenum contour defines an elliptical zone that is elongated north-northeast. The 0.03 percent molybdenum contour defines a nearly closed elliptical annular zone 200 by 360 m wide around a low-grade core. Grades within the 0.03 percent molybdenum zone are variable, with some areas greater than 0.06 percent molybdenum common. The distribution of molybdenum in the ore zone and in the low-grade core are further emphasized in Figure 26.3*B* (based on blast-hole and drill-hole assays).

The maximum depth of molybdenum mineralization is unknown. Using assay data from 19 drill holes, all greater than 300 m total depth, the lower limits of molybdenum mineralization can be approximated. Based upon the 0.03 percent molybdenum contour as an indication of the bottom of molybdenum mineralization, an approximate lower limit of mineralization occurs at the 870-m elevation (365 m below the lowest pit level in 1980). However, several deep, "root-like" zones extend to at least the 536-m elevation. Grade cross sections to the 1188-m elevation indicate that grade contours are nearly vertical (see Fig. 26.3*B*). Figure 26.8 is a schematic diagram of the best approximation of the vertical extent of molybdenum mineralization at Mineral Park, based on the 0.03 percent molybdenum cutoff. It is emphasized that grades greater than 0.02 percent molybdenum occur locally to an elevation of 158 m below sea level.

The lateral extent of hypogene copper mineralization is not well defined because of supergene effects. The hypogene copper grades presented in Figure 26.6 are based on assay values below the last noted occurrence of chalcocite in drill logs. Within the area of Figure 26.6, copper grades range from 0.05 to 0.15 percent and average 0.069 percent. A low-grade copper core (less than 0.05%) coincides with the low-grade molybdenum core. Primary copper grades decrease with depth, but they bottom at higher elevations than molybdenum grades.

The low-grade cores for both molybdenum and copper mineralization coincide. Coexistence of such low-grade cores have been documented in many porphyry copper deposits (Lowell and Guilbert, 1970). At Mineral Park the low-grade core is not centered on exposed Laramide rocks, but is located partly in quartz porphyry and partly in amphibolite

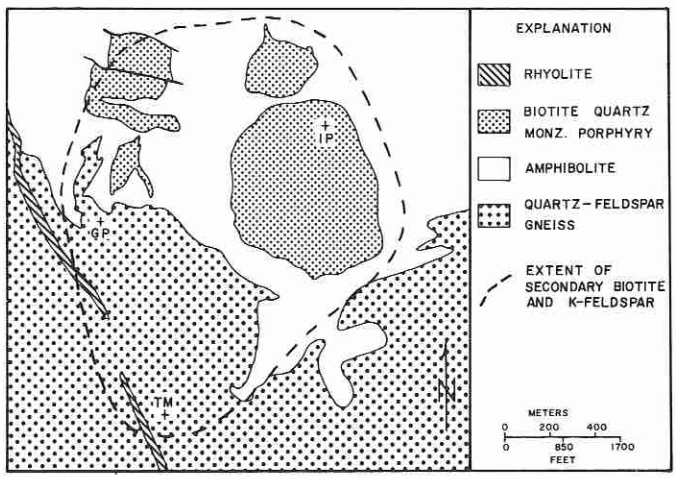

Figure 26.6. Distribution of alteration biotite and K-feldspar at Mineral Park. Key: *GP* = Gross Peak, *IP* = Ithaca Peak, *TM* = Turquoise Mountain.

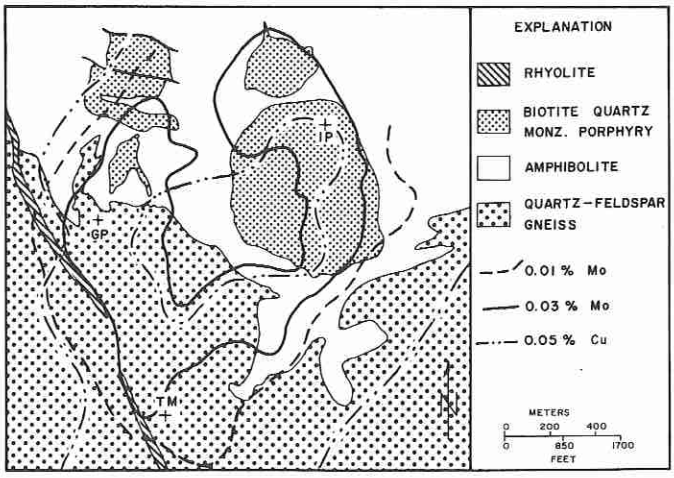

Figure 26.7. Distribution of molybdenum and copper grades at Mineral Park. Key: *GP* = Gross Peak, *IP* = Ithaca Peak, *TM* = Turquoise Mountain.

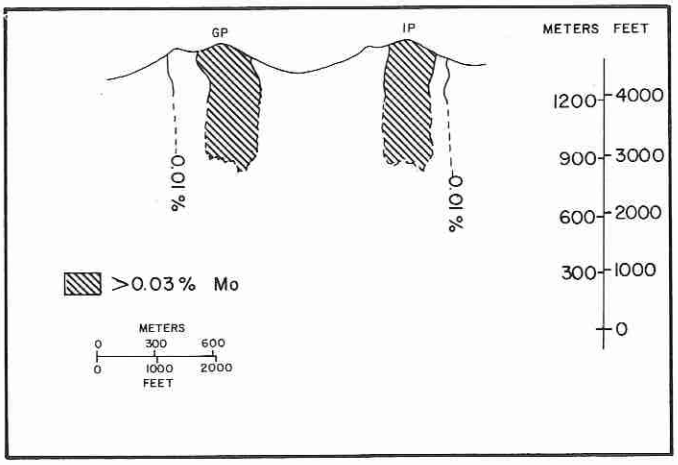

Figure 26.8. Approximate vertical distribution of molybdenum at Mineral Park (looking north). Key: *GP* = Gross Peak, *IP* = Ithaca Peak.

schist (see Fig. 26.7). The quartz porphyry within the core consists of heavily quartz-veined rock and includes the zone of quartz pods and crenulated quartz veins described earlier. Similar quartz-rich cores have been described at OK Tedi, Papua New Guinea (Bamford, 1972) and at Yandera, Papua New Guinea (Titley et al., 1978; Watmuff, 1978).

Copper mineralization has a greater lateral extent than molybdenum (see Fig. 26.7). Diamond drill holes around the eastern and southern margins of the deposit indicate that 0.05 percent copper values extend beyond the 0.01 percent molybdenum contour. Molybdenum values in these same drill holes indicate 0.001 percent molybdenum or less. The district-wide zoning pattern developed from production data on all mines in the Wallapai mining district shows that a central copper-molybdenum zone passes outward into a copper zone, then into a lead-zinc zone, and finally into a peripheral gold-silver zone (Fig. 26.9).

Hypogene copper and molybdenum grades show distinct differences when considered relative to rock type (Table 26.6). Noticeably higher copper grades tend to occur more in the Precambrian mafic rocks than in the more felsic rocks, and molybdenum grades tend to be slightly higher in the more felsic rocks. Molybdenum is almost totally restricted to quartz veins, whereas much of the chalcopyrite is observed in selvages adjacent to veins, where it shows an affinity for mafic mineral sites, especially biotite. This occurrence is consistent with other deposits, such as Ray, where "iron-rich rocks are much better hosts for copper mineralization . . . than are the siliceous rocks . . ." (Phillips et al., 1974, p. 1249).

FRACTURE ORIENTATIONS AT THE MINERAL PARK MINE

Studies of fracturing by Rehrig and Heidrick (1972) have shown that fracture orientations are more complex at Mineral Park than at the other deposits they have studied. Orientations for all mineralized fractures recorded from the mine are shown in Figure 26.10. No single major trend is apparent. Rehrig and Heidrick (1972) have suggested that this lack of

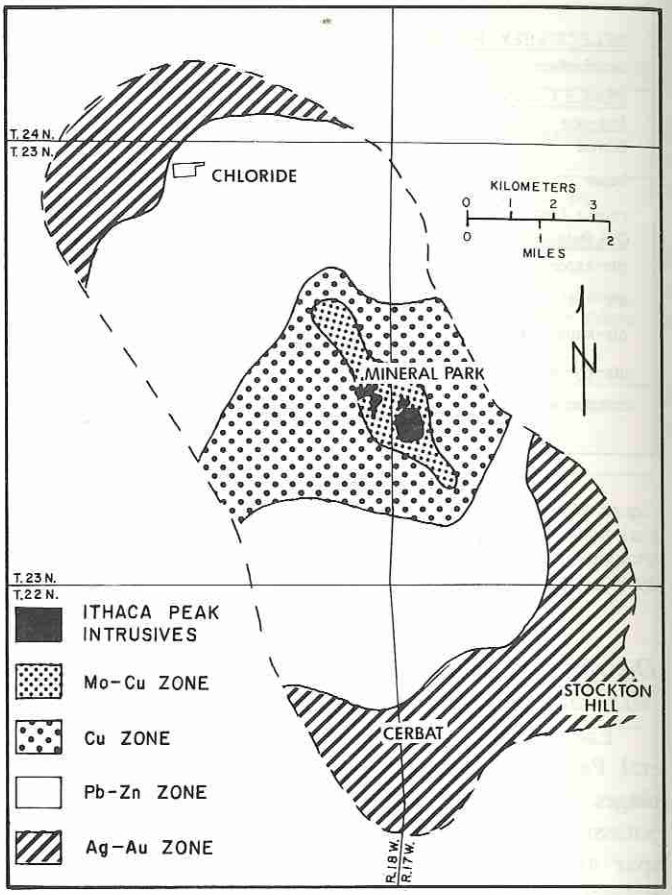

Figure 26.9. Metal zoning of Wallapai mining district, based on production figures for the entire district

TABLE 26.6
Average Grades of Hypogene Copper and Molybdenum by Rock Type at Mineral Park Mine

Rock Type	Cu Grade* (%)	Number of Cu Analyses	Mo Grade* (%)	Number of Mo Analyses
Amphibolite	0.089	376	0.038	390
Hornblende Metadiorite	0.079	245	0.043	245
Quartz Feldspar Gneiss	0.060	713	0.053	714
Biotite Quartz Monzonite Porphyry	0.067	394	0.049	396
Quartz Porphyry	0.065	713	0.039	782

NOTE: Assays by Duval Corporation.
* Grades are for 10-ft. intervals of diamond drill core samples.

systematic orientations might indicate a radial pattern for fracturing at Mineral Park, but continuing studies of the nature of fracturing at Mineral Park have shown that such a radial pattern is not real.

The results of fracture studies in which vein paragenesis is also considered clearly show a change in mineralized fracture orientations with time from oldest to youngest. The molybdenite veinlets at the mine (Fig. 26.11*A*), which are paragenetically early, are characterized by a dominant east-west strike, which reflects no pre-Laramide structural event

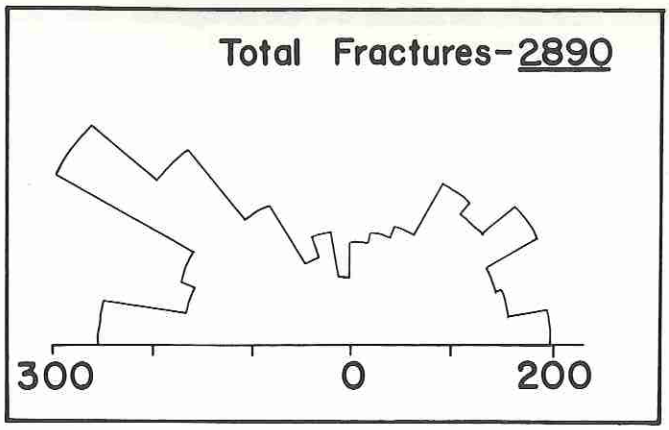

Figure 26.10. Strike diagram of all mineralized fractures at the Mineral Park mine

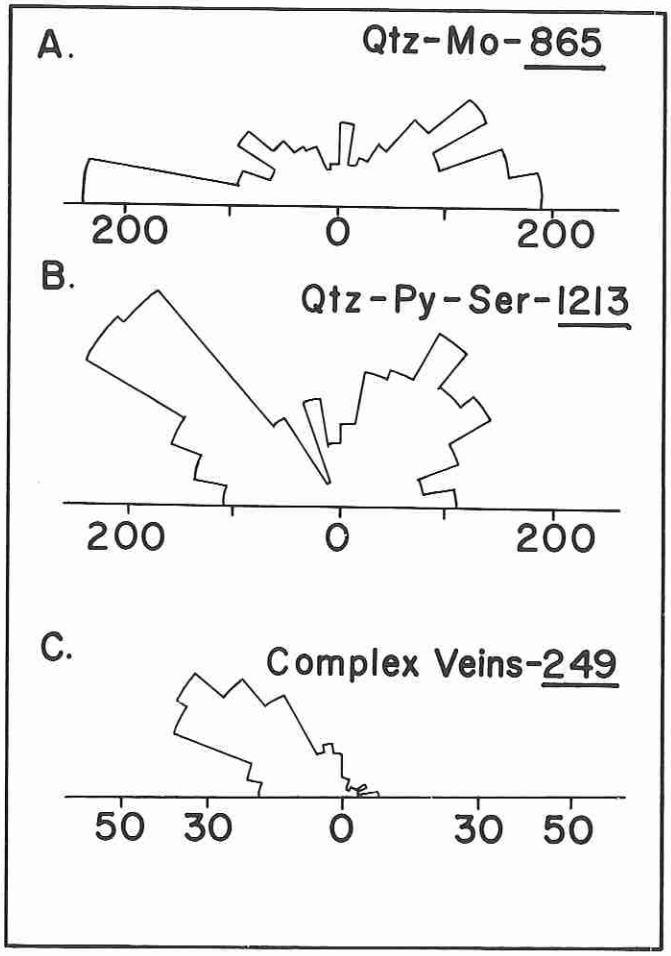

Figure 26.11. Strike diagrams of three types of mineralized fractures at the Mineral Park mine, from oldest to youngest: *A,* quartz-molybdenite *(Qtz-Mo)* veinlets; *B,* quartz-pyrite-sericite *(Qtz-Py-Ser)* veinlets; and *C,* complex sulfide veins.

recognized in the Cerbat Mountains. Two subordinate peaks with strikes of N50 to 60°E and N50 to 60°W are sub-parallel to foliation in the younger Precambrian gneisses and to the Precambrian contact and major fault-veins, respectively. The magnitude of fracturing during the molybdenite stage of mineralization indicated by fracture densities (Titley, 1982) in the ore zone ranges from 0.02 to 0.14 cm^{-1} and it averages 0.05 cm^{-1}.

The quartz-pyrite-sericite veinlets, which cut and are, therefore, younger than the quartz-molybdenite veinlets, show a well-west strike (see Fig. 26.11*B*). Both the northwest and northeast directions are sub-parallel to major structural elements in the Cerbat Mountains. Fracture densities for quartz-pyrite-sericite veinlets in the pit range from 0.05 to 0.33 cm^{-1} (average 0.14 cm^{-1}), which is significantly greater than densities for molybdenum veinlets. Quartz-pyrite-sericite veinlets also extend over a wider area than the quartz-molybdenite veinlets.

The northwest-dominant fracture direction continued during the formation of the paragenetically late complex sulfide veins, and, as Figure 26.11*C* shows, there were no other important fracture directions during the time of their formation. By the time of quartz-pyrite-sericite and complex sulfide vein formation, fractures had evolved from veinlets to major faults, some of which are traceable for over 1.6 km. The fault-vein area extends well beyond the limits of quartz-pyrite-sericite veinlets and defines the 20-km-long Wallapai mining district. The orientation and extent of these fault veins away from the intrusion center at Mineral Park was controlled by the northwest-striking Precambrian boundary in the area.

FLUID INCLUSIONS AT THE MINERAL PARK MINE

Standard fluid inclusion heating and freezing tests were performed on selected vein types in the paragenetic sequence at the Mineral Park mine (Wilkinson, 1980). Reported here are the results of 816 homogenization temperatures and 68 freezing temperatures which were determined from inclusions in quartz intergrown with sulfides in veins representative of the different paragenetic stages. Fluid inclusion analyses were performed after the paragenetic sequence had been established.

An inclusion study by Drake (1972) reported homogenization temperatures from 425 to 450°C in nearly every vein stage; because of mechanical limitations, these temperatures were estimated, rather than measured. The results presented here from the same vein types show that these estimated temperatures were too high.

Two types of fluid inclusions (classifications based on Nash [1976]) were observed at the Mineral Park mine: Type I (liquid-rich inclusions with a vapor bubble and occasional non-halite daughter minerals) and Type III (liquid-rich inclusions with a vapor bubble and a halite daughter mineral).

Type I Inclusions

Type I inclusions are by far the most abundant type observed; they account for 99 percent of the total. They are typically less than 40 μm in average diameter, and most are secondary inclusions occurring along obvious planes. Most of the Type I inclusions consist only of an aqueous liquid and vapor bubble, but occasionally these inclusions contain a birefringent, round or rod-shaped daughter mineral (anhydrite), a reddish opaque phase (hematite), or a

triangular-shaped opaque mineral (chalcopyrite?). Multiple daughters are rare. None of the daughter minerals in Type I inclusions changes or dissolves with heating.

Type III Inclusions

Type III fluid inclusions contain an aqueous liquid and a vapor bubble plus a cubic daughter mineral (halite), which disappears upon heating. Only 25 Type III inclusions were recognized and they were observed only in a coarse-grained quartz-biotite vein. Within this vein they occurred only in quartz that was intricately intergrown with biotite; thus, the inclusions are considered co-depositional with the biotite. Several of the Type III inclusions contained rounded, nonbirefringent daughter minerals initially presumed to be sylvite; this presumption was proved incorrect, however, since the minerals did not change size up to homogenization temperatures. A reddish, opaque (hematite) daughter was occasionally present in Type III inclusions, but no chalcopyrite was observed.

Salinities

Salinities for Type I inclusions were calculated from freezing point depressions, as described by Roedder (1972) and Potter and others (1977*a*). In Type III inclusions, NaCl dissolution always occurred before homogenization to the liquid phase, and their salinities were obtained from the temperature of salt dissolution upon heating by using the NaCl solubility data of Potter and others (1977*b*). The distribution of salinities for both types of inclusions is shown in Figure 26.12. Many workers at other deposits have reported two clearly distinct groups of salinities (Roedder, 1971; Nash, 1976; Preece and Beane, in press; Bodnar and Beane, 1980; Reynolds and Beane, 1979). There is no overlap between the two groups present at Mineral Park: Type III inclusions have salinities which group tightly between 31 and 35 weight percent NaCl equivalent, and Type I inclusions have a somewhat wider range of from 1 to 13 weight percent NaCl equivalent. The high salinity fluids are the earliest fluids observed at Mineral Park.

Homogenization Temperatures

Fluid inclusions, abundant in all vein types at the Mineral Park mine, occur mostly as secondary inclusions along planes. An attempt was made initially to distinguish primary from secondary inclusions, but the ambiguities were such that no clearcut distinction could be made. Instead, at least 50 inclusions were analyzed in samples of each vein type in order to establish statistically valid homogenization temperature distributions. Unique peaks of homogenization temperatures were considered characteristic of given vein sets as defined for other deposits by Preece and Beane (in press) and Bodnar and Beane (1980). Histograms of homogenization temperatures for each vein type are presented in paragenetic order in Figure 26.13.

The quartz pods show a unique peak of homogenization temperatures at 350 to 370°C. The quartz pods are spatially restricted to the core of the quartz porphyry, and, since inclusions of this temperature are not seen elsewhere, the fluids forming the quartz pods may have been equally as

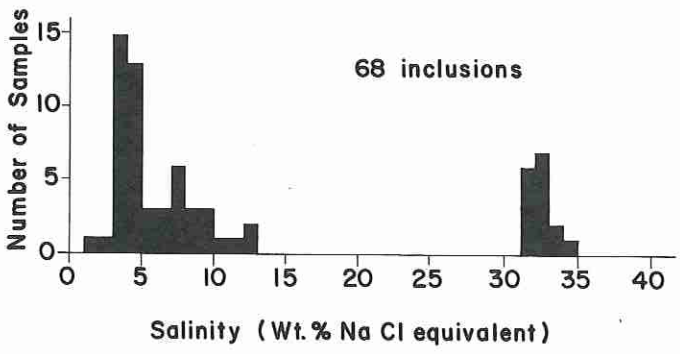

Figure 26.12. Histogram of fluid salinities from all vein types at the Mineral Park mine: *left,* Type I inclusions; *right,* Type III inclusions.

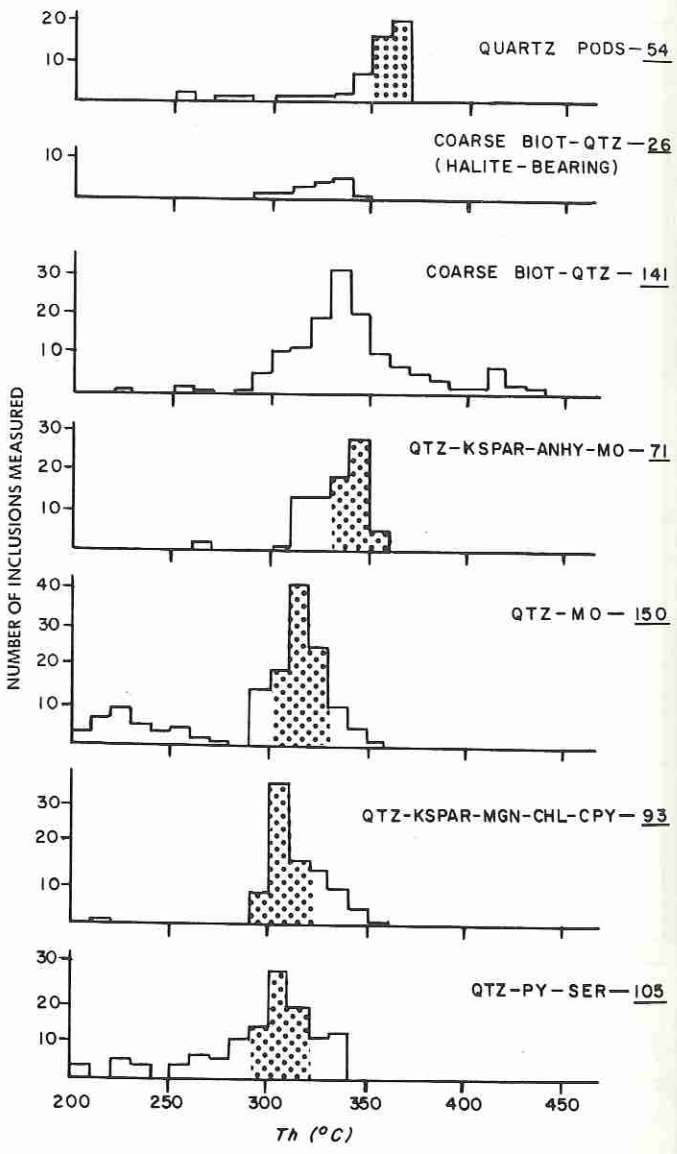

Figure 26.13. Histograms showing distribution of homogenization temperatures for quartz in veinlets (in paragenetic order) at the Mineral Park mine. Numbers of samples tested are shown to the right of each veinlet type. Shaded areas represent unique peaks of temperature. Key: *ANHY* = anhydrite, *BIOT* = biotite, *CHL* = chlorite, *CPY* = chalcopyrite, *KSPAR* = K-feldspar, *MGN* = magnetite, *MO* = molybdenite, *PY* = pyrite, *QTZ* = quartz, *SER* = sericite.

restricted. Their restricted position in the center of the quartz porphyry suggests that the quartz pods preceded other, more widespread vein types. The quartz pods do not record to any extent the fluids from the sulfide-bearing veins. However, occasional sulfides occur along clear quartz veinlets cutting the quartz pods. Homogenization temperatures from these clear quartz veinlets indicate a relationship with fluids of the major sulfide-bearing vein fluids.

The coarse-grained quartz-biotite veins record the most complex fluid evolution of any of the veins examined. Type III inclusions, which were identified as primary, occur only intergrown with biotite and quartz and, thus, can be considered co-depositional with the biotite and quartz. The inclusions in the 410 to 440°C peak of low-salinity fluids occur in quartz not intergrown with biotite; this quartz was introduced later than the biotite. The lower homogenization temperature peak, 300 to 380°C, corresponds to homogenization temperatures of fluids occurring in later sulfide-depositing events. Thus, in the pegmatitic quartz vein there is evidence for an early, moderate-temperature, high-salinity fluid followed by a fluid with a decrease in salinity and increase in homogenization temperature. The same type of sequence has been observed at Sierrita by Preece (1979).

Two unique homogenization temperature peaks occur in molybdenite-bearing veinlets. The 340 to 350°C peak corresponds to quartz–K-feldspar–anhydrite–molybdenite veinlets and the 310 to 330°C peak corresponds to quartz-molybdenite veinlets. The histograms of homogenization temperature peaks for the two vein types are sufficiently different to provisionally define two stages of molybdenum mineralization distinguished from each other by temperature as well as by characteristic alteration assemblages. The quartz-Kspar-chalcopyrite and quartz-pyrite-sericite veinlets have homogenization temperature peaks that are indistinguishable, except that the quartz-chalcopyrite peak is skewed toward higher temperatures and the quartz-pyrite-sericite peak tails off to low temperatures.

All of the vein types observed show evidence for one or two thermal events around 250°C, but these events were well documented in only two samples—quartz phenocrysts and quartz-molybdenite. In all the other samples a brief search was made to insure the presence of such fluid inclusions, but once established, large numbers of homogenization temperatures were not measured; therefore, the number of data in the 200° to 300°C range is small. Because these thermal events were never recognized as unique peaks, the vein assemblages they represent are unknown.

Figure 26.14 is a plot of measured homogenization temperatures versus time for the paragenetic sequence of mineralizing events studied at the Mineral Park mine. There is an early, moderate-temperature, high-salinity event recorded by the pegmatitic quartz. The high-salinity fluids give way abruptly to low-salinity fluids (see Fig. 26.12), the earliest of which shows an increase in homogenization temperature to approximately 420°C. Once the low-salinity fluids predominate, there is a gradual decrease in homogenization temperatures from 420 to 220°C with time. This same sequence of moderate-temperature, high-salinity fluids giving way to higher-temperature, lower-salinity fluids has previously been noted by Preece (1979) at Sierrita.

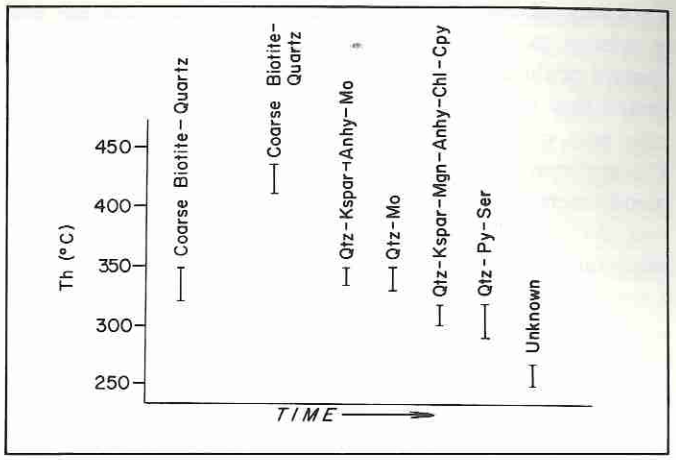

Figure 26.14. Homogenization temperatures vs. time for mineralizing events at Mineral Park

It is important to note that homogenization temperatures during the time of major sulfide deposition varied by only 50°C (from 350 to 300°C). This temperature range represents an almost isothermal temperature regime in which vein alteration assemblages evolve from K-feldspar–biotite stability to K-feldspar–chlorite stability to sericite-chlorite stability, with subsequent deposition of the economic sulfide mineralization at Mineral Park. The nearly isothermal conditions during sulfide deposition and the evolution of alteration assemblages have also been noted by Preece (1979) and by Reynolds (1980) at Santa Rita

In his study of Mineral Park, Drake (1972) has not reported any evidence for boiling; Drake and Ypma (1969) have reported that boiling took place during the chalcopyrite stage, but their evidence was not presented. During the course of this study, no evidence for boiling was observed and no inclusions homogenized to the vapor phase. Since boiling was not indicated at Mineral Park, only minimum pressures can be established for vein formation. Minimum pressure varied considerably during the regime of low-salinity fluids —from approximately 360 to 80 bars. Minimum pressures during sulfide deposition varied from 180 to 80 bars. These pressures correspond to minimum depths of formation of 2 to 3 km. These figures agree well with depths of burial of approximately 3 km, based on restored stratigraphy from the adjacent Colorado Plateau. Because boiling did not occur, a pressure correction is required to obtain trapping temperatures. At a constant pressure (250 bars) and salinity (10 weight % NaCl equivalent), the magnitude of this correction ranges from +10 to +25°C, with the larger value corresponding to lower homogenization temperatures (Potter, 1977).

DISCUSSION

The formation of the Mineral Park deposit reflects the interaction of different geologic events over time: events such as structural setting, intrusion, timing and degree of fracturing, and chemical and structural controls of mineralization acted in concert to produce the deposit being mined.

Structural relationships among rocks in the district provide evidence for interpreting the localization of the Mineral

Park deposit. Because mineralization is of Laramide age and is related to Laramide intrusions, its location reflects the control of the Laramide intrusions. Thomas (1953) has suggested that the emplacement of the Diana Granite at Chloride was controlled by the Chloride Fold, which is of Precambrian age. The nature of the distribution of hornblende metadiorite at the mine suggests that its emplacement was also controlled by a Precambrian fold—the Turquoise Mountain fold. Thus, in Precambrian time, folding served as a structural control for intrusions.

The contact between older and younger Precambrian rocks appears to have exerted an important control over the localization of Laramide intrusions and mineralization. The Ithaca Peak stock and Alum Wash mineralized area are aligned along a northwest trend which is parallel to the strike of the majority of rhyolite dikes in the district. It seems more than coincidental that these northwest trends are also parallel to the recognized Precambrian contact. Furthermore, both mineralized areas occur near intersections of the Precambrian contact and major folds: Alum Wash near the Roper Ridge fold and Ithaca Peak near the Turquoise Mountain fold. These relationships suggest that the emplacement of Laramide intrusions was guided by Precambrian structure and localized at the intersection of folds and the contact between the two Precambrian domains.

A close genetic link between the Mineral Park mine and the veins of the Wallapai mining district is apparent from zoning of different phenomena. Mineral Park occurs at the approximate geographic center of the district. Complex copper-lead-zinc-silver veins are paragenetically late in the mine area. Data presented by Drake (1972) have suggested a thermal link between porphyry copper and vein mineralization. Homogenization temperatures in the complex base-precious metal veins of the district range from 186 to >360°C; the majority of the veins have measured homogenization temperatures from 290 to 350°C. The fluids from these veins have low salinities, ranging from 1 to 4.7 weight percent NaCl equivalent. These fluids are nearly identical to sulfide-depositing fluids recognized in the mine.

Production data acquired from all the veins in the Wallapai mining district have been used to develop zoning maps based on metal ratios. The resulting zoning picture is not as symmetrical as that of Eidel and others (1968), but does show pronounced zoning from a molybdenum-copper zone centered at Mineral Park outward to an intermediate lead-zinc zone and finally to a peripheral gold-silver zone.

The occurrence of Mineral Park at the geographic center of the vein deposits, the metal zoning around the mine, the paragenetic relationships between porphyry copper and vein mineralization, and the similarity of thermosaline properties of the fluids from porphyry copper and vein mineralization strongly indicate a genetic relationship between mineralization at Mineral Park and vein mineralization throughout the district. It is suggested here that the Alum Wash and Mineral Park mineralized areas represent apophyses from a northwest-trending batholith and that the extent of this batholith is outlined by the lateral extent of dikes and veins.

Significant data for interpreting the environment of formation of the ore deposit at Mineral Park are provided by fluid inclusion analyses and by the distribution of mineralization. Fluid inclusion data and reconstructed stratigraphic columns yield a minimum depth of formation of mineralization of approximately 3 km. This is consistent with depths of formation interpreted for many other porphyry copper deposits (Lowell and Guilbert, 1970).

The narrow range of homogenization temperatures (250–440°C) spanning the life of the ancient geothermal system at Mineral Park and the lack of high homogenization temperatures constrain the temperature range and the environment of ore formation. Perhaps the best explanation for the lack of high-temperature fluids at Mineral Park can be found in the numerical simulation studies of Norton and Knight (1977) and Norton (1979). Such studies indicate that high temperatures (>500°C) are characteristic of the immediate pluton environments and occur for only short periods of time. This interpretation is consistent with fluid inclusion results from intrusion-centered deposits such as Bingham (Roedder, 1971; Nash and Cunningham, 1974) and Santa Rita (Reynolds, 1980), where homogenization temperatures greater than 700°C are observed in early veins.

There is a broad vertical region several kilometers high above the cooling pluton—the lithocap region (Norton, 1979)—where temperatures of 200 to 300°C were reached and maintained for long periods of time during the history of the cooling pluton. Norton's results are based on calculations using properties of pure water. The addition of NaCl to the fluid causes a shift—towards higher temperatures—of heat and transport properties of the fluid which would increase temperatures up to the 400°C range above the pluton (Norton, 1979). It is significant that this is the same range (200°C to 400°C) of homogenization temperatures observed at Mineral Park; it is also the same range of homogenization temperatures observed by Bodnar (1978) at Red Mountain in a lithocap environment where the intrusion is unknown.

The lateral extent of both copper and molybdenum mineralization defines an annular zone with a low-grade core. The vertical extent of molybdenum mineralization defines a nearly vertical cylinder which bottoms at approximately the 2,800-ft. elevation; anomalous molybdenum is present to the greatest depths drilled. The distribution of copper and molybdenum with respect to rock types shows that ore-grade mineralization is equally distributed between Laramide- and Precambrian-age rocks, with ore zones cutting across lithologic contacts. There is little suggestion of mineralization zoning relative to exposed Laramide rocks.

The distribution of alteration and mineralization, the narrow range of homogenization temperatures (comparable to predicted results from theoretical modeling), and the lack of high homogenization temperatures suggest that mineralization events at Mineral Park are not related to exposed Laramide rocks. Using Norton's modeling (1979) it can be interpreted that mineralization formed from 1 to 3 km above the causative pluton, but not adjacent to or within the causative pluton. The order of fluid salinities observed at Mineral Park—early high salinity followed by low salinity—is the opposite of that observed by Bodnar (1978) in the lithocap region at Red Mountain.

An important question concerns how deep the buried

source is and whether there might be intrusion-centered mineralization associated with it. Two deep holes were drilled, one to a depth of 1.524 km near the outer edge of the low-grade core, and the other to a depth of 762 m near the center of the low-grade core. Neither encountered evidence for different mineralization zones nor evidence for another intrusive phase. It appears that the causative pluton and possible associated mineralization are very deep.

The controls of mineralization at the Mineral Park deposit consist of a combination of structural and chemical factors. Certain gross structural controls are evident, and it is clear that mineralization was deposited in and adjacent to fractures. The western edge of molybdenum mineralization is controlled to a large degree by the rhyolite-filled Gross Peak fault. The molybdenum grade contours decrease adjacent to the fault and parallel it southward to Turquoise Mountain. The tail in the 0.03 percent molybdenum contour on Turquoise Mountain suggests that mineralizing fluids were trapped against the fault and channeled along it to the south for a short distance. To the east, molybdenum mineralization ceases abruptly at the biotite quartz monzonite porphyry–Precambrian contact. Fracture densities show that the abundance of molybdenite veinlets drops to zero near this contact, although total densities—especially of quartz-pyrite-sericite veinlets—remain high (0.1–0.3 cm^{-1}); the scarcity of quartz-chalcopyrite veinlets prevents a similar analysis for the copper-forming event. Figure 26.7 shows that copper mineralization does extend beyond molybdenum mineralization and, to the west, even crosses the Gross Peak fault. To the east, alteration and mineralization effects die very quickly at or near the Precambrian boundary; there is also a pronounced drop in fracture densities at this boundary, with only quartz-pyrite-sericite veinlets observed east of it.

The distribution of molybdenum grades indicates that the density of molybdenum-bearing fractures must be lower in the low-grade core than in the ore zone. When the shape and position of the annular ore zone is compared to rock types, a significant pattern emerges. The high-grade molybdenum zone (zone of high fracture denisty) occurs largely in quartz monzonite porphyry and quartz-feldspar gneiss, with only minor amounts in the amphibolite schist. The quartz monzonite porphyry and quartz-feldspar gneiss are more susceptible to brittle fracture than is the amphibolite, and they have developed higher fracture densities. The low-grade core can, therefore, be attributed to a combination of poor fracturing characteristics of the amphibolite and the presence of the quartz-rich porphyry. The annulus of mineralization developed in response to different mechanical properties of the various rock types and/or to different stress mechanisms, coupled with changes in the magnitude of strain, which resulted in fracturing.

Chemical controls are less obvious than fracture controls, but they played a major role in sulfide ore deposition. The narrow range of homogenization temperatures measured for different alteration-mineralization events suggests that temperature change was not a major control during sulfide deposition. Ore deposition occurred under nearly isothermal conditions in response to changes in fluid composition manifested by changes in alteration assemblages. The most important chemical control appears to have been changes in the hydrothermal fluid due to water-rock interactions. These chemical changes can be traced through the use of the activity diagram in Figure 26.15. Equilibrium of early fluids with K-feldspar and biotite resulted in the deposition of both minerals in veinlets and left primary K-feldspar and biotite unaffected adjacent to veinlets (see section *A* in Fig. 26.15). Molybdenum deposition occurred near the end of this assemblage. Following molybdenum mineralization, the fluids changed (see section *B,* Fig. 26.15): K-feldspar was still stable, but biotite was altered to chlorite, due to decreasing a_{K^+}/a_{H^+} or to the increasing acidity of the fluid (Beane, 1982). Further increases in acidity then drove the fluid composition into equilibrium with sericite and chlorite (see section *C,* Fig. 26.15), and pyrite became the dominant sulfide mineral. It should be emphasized again that these fluid changes were occurring at essentially isothermal conditions starting at approximately 350°C and ending at 300°C.

Sulfide mineralization decreases with depth, though fracturing persists. The potassic assemblage, K-feldspar–biotite–anhydrite, becomes more abundant with depth and sulfides decrease, copper more rapidly than molybdenum. Molybdenite veinlets from 1.524 km deep yield homogenization temperatures equal to those from the surface (±330°C); however, when temperature corrections are made for the increase in depth, the homogenization temperature rises to approximately 400°C. At such a temperature, sulfides were not a major component of veinlets, and they became so only with the deposition of molybdenite at approximately 350°C. The increase in temperature with depth may have driven hydrothermal fluids into the potassic assemblage stability fields,

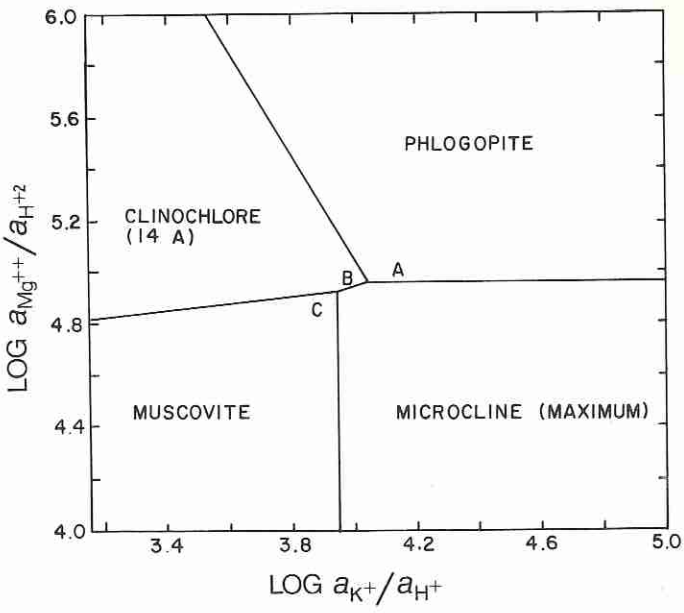

Figure 26.15. Activity diagram showing fluid evolution during mineralization at Mineral Park from the earliest fluids at *A* to the latest fluids at *C*. Diagram is constructed at 300°C and 300 bars pressure. The diagram is balanced on Al^{+3} in the presence of excess SiO_2 and H_2O. The stability field of biotite takes solid solution into account in order to permit stability with K-feldspar, and the chlorite stability field is schematically drawn to depict compatibility with K-feldspar, as suggested for pure phases at 300°C. After Beane (1982).

where sulfides were not abundant. Temperature, then, may have exerted a major control on the vertical distribution of sulfide mineralization.

ACKNOWLEDGMENTS

The authors wish to thank the Duval Corporation for permission to publish this study and for financial support for one author (WHW) during his dissertation (Wilkinson, 1980) research. In particular, the interest and strong support of W. J. Roper, former Resident Manager, and G. P. Boone, Chief Engineer, during the research phase of this study and the continued support of M. R. Miller, Resident Manager, are gratefully acknowledged. Dr. J. I. Sharpe and R. A. Metz, of the Duval Exploration Department, were most helpful with time, logistical support, and critical discussions. Many of the geological data presented in this chapter were collected by many mine geologists at Mineral Park. The help and guidance given by Drs. R. E. Beane, G. A. Davis, J. M. Guilbert, and D. L. Norton of the University of Arizona during the dissertation research are also gratefully acknowledged.

REFERENCES CITED

Bamford, R. W., 1972, The Mount Fubilan (OK Tedi) porphyry copper deposit, Territory of Papua and New Guinea: Econ. Geol., v. 67, p. 1019–1033.

Beane, R. E., 1982, Hydrothermal alteration in silicate rocks, *in* Titley, S. R., ed., Advances in Geology of the Porphyry Copper Deposits, Southwestern North America: Tucson, Univ. Ariz. Press, Chapter 6.

Bodnar, R. J., and Beane, R. E., 1980, Temporal and spatial variations in hydrothermal fluid characteristics during vein filling in pre-ore cover overlying deeply-buried porphyry copper mineralization at Red Mountain, Arizona: Econ. Geol., v. 75, p. 876–893.

Brimhall, G. H. Jr., 1977, Early fracture-controlled disseminated mineralization at Butte, Montana: Econ. Geol., v. 72, p. 37–59.

Carson, D. J. T., and Jambor, J. L., 1974, Mineralogy, zonal relationships, and economic significance of hydrothermal alteration at porphyry copper deposits, Babine Lake area, British Columbia: Can. Min. Metall. Bull., v. 67, p. 110–133.

Dings, M. G., 1951, The Wallapai mining district, Cerbat Mountains, Mohave County, Arizona: U.S. Geol. Survey Bull. 978-E, p. 123–163.

Drake, W. E., 1972, A study of ore-forming fluids at the Mineral Park porphyry copper deposit, Kingman, Arizona: Unpub. Ph.D. Diss., Columbia Univ., 245 p.

Drake, W. E., and Ypma, P. J. M., 1969, Fluid inclusion study of the Mineral Park porphyry copper deposit, Kingman, Arizona: *in* Roedder, E., ed., Proc. of COFFI, 1969, vol. 2, p. 15.

Eidel, J. J.; Frost, J. E.; and Clippinger, D. M., 1968, Copper-molybdenum mineralization at Mineral Park, Mohave County, Arizona, *in* Ridge, J. D., ed., Ore Deposits of the United States 1933–1968: New York, A.I.M.E., p. 1259–1281.

Graybeal, F. T., 1972, The partition of trace elements among coexisting minerals in some Laramide intrusive rocks in Arizona: Unpub. Ph.D. Diss., Univ. Ariz., 220 p.

Kessler, E. J., 1976. Rubidium-strontium geochronology and trace element geochemistry of Precambrian rocks in the northern Hualapai Mountains, Mohave County, Arizona: Unpub. M. S. Thesis, Univ. Ariz., 73 p.

Lowell, J. D., and Guilbert, J. M., 1970, Lateral and vertical alteration-mineralization zoning in porphyry ore deposits: Econ. Geol., v. 65, p. 373–408.

Mauger, R. L., and Damon, P. E., 1965, K-Ar ages of Laramide magmatism and copper mineralization in the Southwest: Atomic Energy Comm. Annual Progress Report No. C00-689-50, p. A-II-1–A-II-8.

Nash, J. T., 1976, Fluid inclusion petrology—data from porphyry copper deposits and applications to exploration: U.S. Geol. Survey Prof. Paper 907-D, 16 p.

Nash, J. T., and Cunningham, C. G., 1974, Fluid inclusion studies of the porphyry copper deposit at Bagdad, Arizona: Jour. Res., U.S. Geol. Survey, v. 2, p. 31–34.

Nielsen, R. L., 1968, Hypogene texture and mineral zoning in a copper-bearing granodiorite porphyry stock, Santa Rita, New Mexico: Econ. Geol., v. 63, p. 37–50.

Norton, Denis, 1979, Transport phenomena in hydrothermal systems: the redistribution of chemical components around cooling magmas: Bull. Mineral., v. 102, p. 471–486.

Norton, Denis, and Knight, Jerry, 1977, Transport phenomena in hydrothermal systems: Cooling plutons: Am. Jour. Sci., v. 277, p. 937–981.

Phillips, C. H.; Gambell, N. A.; and Fountain, D. S., 1974, Hydrothermal alteration, mineralization and zoning in the Ray deposit: Econ. Geol., v. 69, p. 1237–1250.

Potter, R. W. Jr., 1977, Pressure corrections for fluid inclusion homogenization temperatures based on the volumetric properties of the system NaCl-H_2O: Jour. Res., U. S. Geol. Survey, v. 5, no. 5, p. 603–607.

Potter, R. W. Jr., Clynne, M. A.; and Brown, D. L., 1977*a,* Freezing point depression of aqueous sodium chloride solutions: Econ. Geol., v. 73, p. 284–285.

Potter, R. W. Jr.; Babcock, R. S.; and Brown, D. L., 1977*b,* A new method for determining the solubility of salts in aqueous solutions at elevated temperatures: Jour. Res., U. S. Geol. Survey, v. 5, no. 3, p. 389–395.

Preece, R. K. III, 1979, Paragenesis, geochemistry, and temperatures of formation of alteration assemblages at the Sierrita deposit, Pima County, Arizona: Unpub. M.S. Thesis, Univ. of Ariz., 106 p.

Preece, R. K. III, and Beane, R. E., in press, Contrasting evolutions of hydrothermal alteration in quartz monzonite and quartz diorite at the Sierrita porphyry copper deposit, Arizona: Econ. Geol., v. 76.

Rehrig, W. A., and Heidrick, T. L., 1972, Regional fracturing in Laramide stocks of Arizona and its relationship to porphyry copper mineralization: Econ. Geol., v. 67, p. 198–213.

Reynolds, T. J., 1980, Variations in hydrothermal fluid characteristics through time at the Santa Rita, New Mexico, porphyry copper deposit: Unpub. M. S. Thesis, Univ. Ariz., 52 p.

Reynolds, T. J., and Beane, R. E., 1979, The evolution of hydrothermal fluid characteristics through time at the Santa Rita, New Mexico, porphyry copper deposit (abs.): Abs. Ann. Mtg. Geol. Soc. America, v. 11, p. 502.

Roedder, E., 1971, Fluid inclusion studies on the porphyry type deposits at Bingham, Utah; Butte, Montana; and Climax, Colorado: Econ. Geol., v. 66, p. 98–120.

———, 1972, Composition of fluid inclusions: U.S. Geol. Survey Prof. Paper 440JJ, 164 p.

Shafiqullah, M.; Damon, P. E.; Lynch, D. J.; Reynolds, S. J.; Rehrig, W. A.; and Raymond, R. H., 1980, K-Ar geochronology and geologic history of southeastern Arizona and adjacent areas: Ariz. Geol. Soc. Digest, v. XII, p. 201-260.

Silver, L. T., 1967, Apparent age relations in the older Precambrian stratigraphy of Arizona (abs.): I.U.G.S. Comm. Geochronology Conf. on Precambrian Stratified Rocks, Edmonton, Canada, p. 87.

Silver, L. T.; Bickford, M. E.; Van Schmus, W. R.; Anderson, J. L.; Anderson, T. H.; and Medaris, L. G., 1977, The 1.4–1.5 B.Y. transcontinental anorogenic plutonic perforation of North America: Geol. Soc. Amer. Abs. with Programs v. 9, no. 7, p. 1176–1177.

Stringham, Bronson, 1966, Igneous rock types and host rocks asso-

ciated with porphyry copper deposits, *in* Titley, S. R., and Hicks, C. L., eds., Geology of the Porphyry Copper Deposits, Southwestern North America: Tucson, Univ. Ariz. Press, p. 35–40.

Thomas, B. E., 1949, Ore deposits of the Wallapai district, Arizona: Econ. Geol., v. 44, p. 663–705.

———, 1953, Geology of the Chloride quadrangle, Arizona: Geol. Soc. of America Bull., v. 64, p. 391–420.

Titley, S. R., 1978, Geologic history, hypogene features, and processes of secondary sulfide enrichment at the Plesyumi Copper Prospect, New Britain, Papua New Guinea: Econ. Geol., v. 73, p. 768–784.

———, 1982, The style and progress of mineralization and alteration in porphyry copper systems, American Southwest, *in* Titley, S. R., ed., Advances in Geology of the Porphyry Copper Deposits, Southwestern North America: Tucson, Univ. Ariz. Press, Chapter 5.

Titley, S. R.; Fleming, A. W.; and Neale, T. I., 1978, Tectonic evolution of the porphyry copper system at Yandera, Papua New Guinea: Econ. Geol., v. 73, p. 810–828.

Wallace, S. R.; Mackenzie, W. B.; Blair, R. G.; and Muncaster, N. K., 1978, Geology of the Urad and Henderson molybdenite deposits, Clear Creek County, Colorado, with a section on a comparison of these deposits with those at Climax, Colorado: Econ. Geol., v. 73, p. 325–368.

Wasserburg, G. J., and Lanphere, M. A., 1965, Age determinations in the Precambrian of Arizona and Nevada: Geol. Soc. of America Bull, v. 76, p. 735–758.

Watmuff, G., 1978, Geology and alteration-mineralization zoning in the central portion of the Yandera porphyry copper prospect, Papua New Guinea: Econ. Geol., v. 73, p. 829–856.

Wilkinson, W. H. Jr., 1981, The distribution of alteration and mineralization assemblages of the Mineral Park Mine, Mohave County, Arizona: Unpub. Ph.D. Diss., Univ. Ariz., 101 p.